J Ind Microbiol Biotechnol (2017) 44:431–441
DOI 10.1007/s10295-016-1898-4

METABOLIC ENGINEERING AND SYNTHETIC BIOLOGY - ORIGINAL PAPER

Metabolic engineering of *Klebsiella pneumoniae* based on in silico analysis and its pilot-scale application for 1,3-propanediol and 2,3-butanediol co-production

Jong Myoung Park[1] · Chelladurai Rathnasingh[1] · Hyohak Song[1]

Received: 16 November 2016 / Accepted: 23 December 2016 / Published online: 31 December 2016

Abstract *Klebsiella pneumoniae* naturally produces relatively large amounts of 1,3-propanediol (1,3-PD) and 2,3-butanediol (2,3-BD) along with various byproducts using glycerol as a carbon source. The *ldhA* and *mdh* genes in *K. pneumoniae* were deleted based on its in silico gene knockout simulation with the criteria of maximizing 1,3-PD and 2,3-BD production and minimizing byproducts formation and cell growth retardation. In addition, the agitation speed, which is known to strongly affect 1,3-PD and 2,3-BD production in *Klebsiella* strains, was optimized. The *K. pneumoniae ΔldhA Δmdh* strain produced 125 g/L of diols (1,3-PD and 2,3-BD) with a productivity of 2.0 g/L/h in the lab-scale (5-L bioreactor) fed-batch fermentation using high-quality guaranteed reagent grade glycerol. To evaluate the industrial capacity of the constructed *K. pneumoniae ΔldhA Δmdh* strain, a pilot-scale (5000-L bioreactor) fed-batch fermentation was carried out using crude glycerol obtained from the industrial biodiesel plant. The pilot-scale fed-batch fermentation of the *K. pneumoniae ΔldhA Δmdh* strain produced 114 g/L of diols (70 g/L of 1,3-PD and 44 g/L of 2,3-BD), with a yield of 0.60 g diols per gram glycerol and a productivity of 2.2 g/L/h of diols, which should be suitable for the industrial co-production of 1,3-PD and 2,3-BD.

Keywords 1,3-Propanediol · 2,3-Butanediol · *Klebsiella pneumoniae* · In silico · Pilot-scale fermentation · 5000-L bioreactor

✉ Hyohak Song
hyohaks@gscaltex.com

[1] Research and Development Center, GS Caltex Corporation, Expo-ro 359, Yuseong-gu, Daejeon 34122, Republic of Korea

Introduction

Bio-based diols, including 1,3-propanediol (1,3-PD; $C_3H_8O_2$) and 2,3-butanediol (2,3-BD; $C_4H_{10}O_2$), are increasingly considered to be promising platform chemicals due to their extensive applications in the commodity and specialty chemical industries. 1,3-PD is well known as a monomer for the synthesis of polytrimethylene terephthalate (PTT), which has excellent properties for textiles, carpets, and fibers [2, 30]. Additionally, 1,3-PD is used for cosmetics, personal care products, solvents, lubricants, preservatives, and drugs [2, 30, 37]. Dehydration of 2,3-BD yields 1,3-butadiene, which is an intermediate for the manufacture of synthetic rubber, and methyl ethyl ketone, which is an effective fuel additive and industrial solvent [3, 8, 37]. Moreover, (*R*,*R*)-2,3-BD, a stereoisomer of (*R*,*S*)-, (*R*,*R*)-, and (*S*,*S*)-forms, is as an effective agent in promoting plants' own defense systems against diseases, drought, and the elements [28, 29].

Both of these diols are produced concurrently by *Klebsiella pneumoniae* during glycerol fermentation [2, 6, 17, 35, 36]. Glycerol is one of the most economic carbon sources for industrial fermentation since it is a massive byproduct of the biodiesel industry, yielding about 10 wt% of biodiesel [5]. *K. pneumoniae* converts glycerol to 3-hydroxypropionaldehyde by a coenzyme B_{12}-dependent glycerol dehydratase via a reductive pathway (Fig. 1). Then, 3-hydroxypropionaldehyde is reduced to 1,3-PD by 1,3-PD oxidoreductases with the oxidation of NADH. On the other hand, an oxidative pathway leads to 2,3-BD production and provides the reducing power for 1,3-PD and 2,3-BD synthesis by generating NADH (Fig. 1). However, various byproducts, including lactic acid, ethanol, acetic acid, succinic acid, and formic acid, formed in the oxidative pathway, lower the yields of the diols by interfering

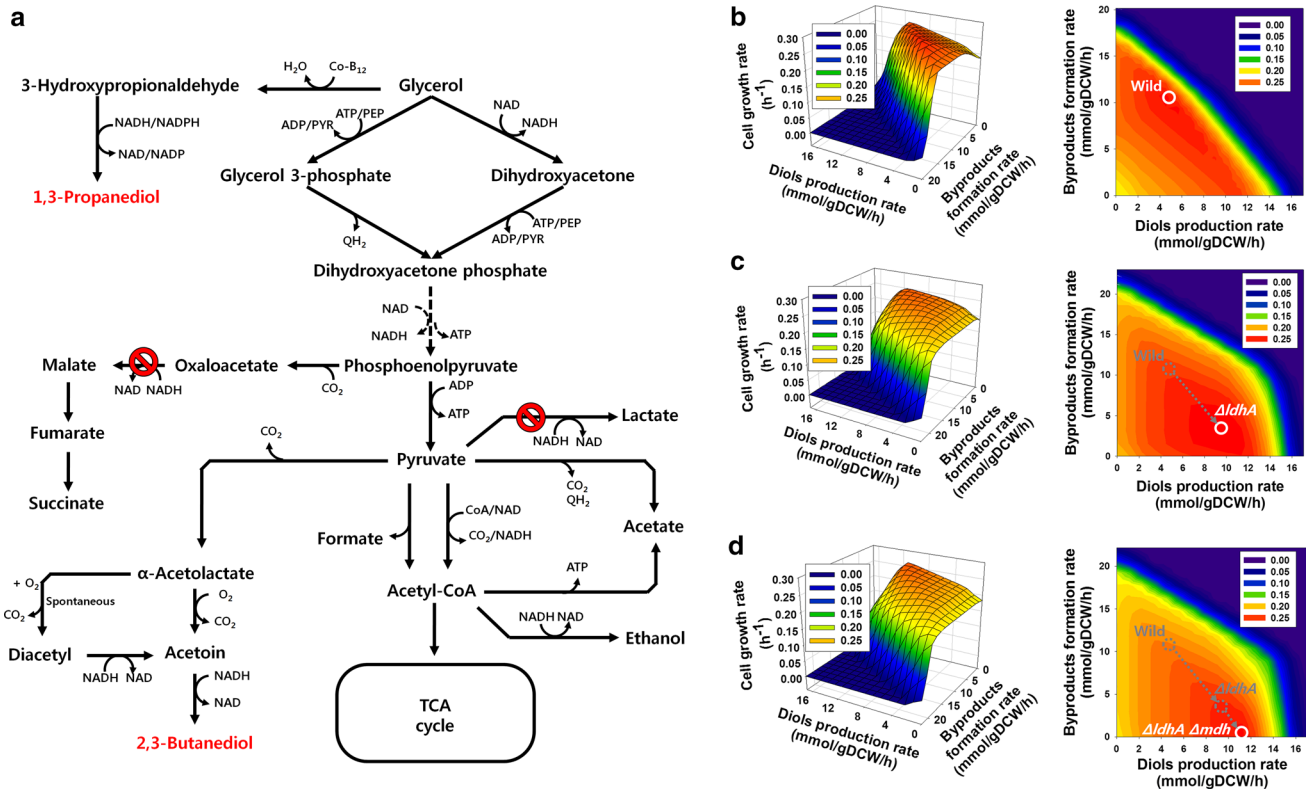

Fig. 1 In silico investigation for flux solution spaces of *K. pneumoniae* wild-type and mutant strains. **a** Schematic metabolic pathway related to 1,3-PD and 2,3-BD production. 3D mesh plot graph as a continuous surface for in silico flux solution spaces of *K. pneumoniae* **b** wild-type, **c** *ΔldhA*, and **d** *ΔldhA Δmdh* strains. The maximal point of in silico cell growth rate is generally acceptable for predicting the actual state of a cell, which is denoted by a *small circle*, because the first priority of an actual cell is survival [21, 22, 31]. The *dotted arrow* indicates the transition of maximal cell growth rate by gene manipulation. The *colors* in the *contour graph* indicate the values of cell growth rate. Byproduct contains ethanol and several organic acids: lactic acid, acetic acid, succinic acid, and formic acid (color figure online)

with the metabolic fluxes toward 1,3-PD and 2,3-BD synthesis. Accordingly, byproducts formation should be decreased while cell growth retardation and redox imbalance are minimized in order to improve the suitability of the *K. pneumoniae* strain for industrial co-production of 1,3-PD and 2,3-BD.

Various genetic modifications of *K. pneumoniae* have been conducted by deleting the genes responsible for the byproducts formation in order to enhance its production of 1,3-PD or 2,3-BD. Deleting the *ldhA* gene encoding lactate dehydrogenase was effective for the enhanced production of both 1,3-PD and 2,3-BD in *K. pneumoniae* [10, 12, 17, 20, 27, 35]. Guo et al. [10] and Rathnasingh et al. [27] reported that the additional deletions of the ethanol dehydrogenase gene (*adhE*) and the phosphotransacetylase gene (*pta*) improved 2,3-BD production. Likewise, Jung et al. [12] significantly increased 2,3-BD yield by the additional inactivation of the pyruvate formate lyase gene (*pflB*). Many researchers have focused on the enhancement of 1,3-PD production by preventing the formation of 2,3-BD and byproducts [4, 14, 38]. For example, Lin et al. (2016) developed a mutant with the genes *poxB* (pyruvate oxidase), *pta* (phosphotransacetylase), and *ackA* (acetate kinase) deleted in order to enhance 1,3-PD production. However, blocking the formation of 2,3-BD and byproducts has a tendency to cause extreme growth retardation. This study focused on developing a strain with enhanced co-production of 1,3-PD and 2,3-BD by reducing byproducts formation without growth retardation. Co-produced 1,3-PD and 2,3-BD can be separated in a downstream process using the differences in their boiling points, 211–217 °C for 1,3-PD and 179–184 °C for 2,3-BD.

We previously isolated a *K. pneumoniae* KCTC12133BP strain that forms few lipopolysaccharide and mucous-like substances, which act as significant virulence determinants [1, 26]. To investigate the complex metabolic network of cells at systems level and to identify gene knockout targets, we used a genome-scale metabolic model of *K. pneumoniae*, iYL1228, and carried out its simulation based on optimization techniques [16]. The performance of genetically engineered mutants was tested in a 5-L bioreactor to determine the optimal fed-batch fermentation condition. Finally,

the pilot-scale fed-batch fermentation in a 5000-L bioreactor using crude glycerol was performed to evaluate the industrial co-production of 1,3-PD and 2,3-BD.

Materials and methods

Genome-scale metabolic model and constraints-based flux analysis

In order to predict the metabolic characteristics produced by genetic perturbations and to identify knockout candidates for 1,3-PD and 2,3-BD co-production, the genome-scale metabolic model of *K. pneumonia*, iYL1228, was used in this study [16]. Constraints-based flux analysis, including flux balance analysis, was carried out under the assumption of a pseudo-steady state [7, 9, 22, 32]. Mass balances in the stoichiometric model can be set up as $S_{ij} \times v_j = 0$, in which S_{ij} is a stoichiometric coefficient of a metabolite i in the jth reaction and v_j is the metabolic flux [mmol/gDCW (gram dry cell weight)/h] of the jth reaction. The in silico model, which is an underdetermined system due to insufficient constraints, can be simulated by optimization techniques including linear programming, subject to the constraints of mass balances, experimental measurements, and thermodynamics as follows:

$$\text{Maximize/minimize } Z = \sum_{j \in J} c_j v_j$$

$$\text{Subject to } \sum_{j \in J} S_{ij} v_j = b_i, \quad \forall i \in I$$

$$\alpha_j \leq v_j \leq \beta_j, \quad \forall j \in J$$

Z indicates objective function, which is usually the maximization of cell growth rate, and c_j is the weight of the reaction j. b_i is the net transport flux of metabolite i, which is zero for intermediate metabolites as in $S_{ij} \times v_j = 0$. α_j and β_j are the lower and upper bounds of the metabolic flux of the jth reaction. For in silico simulations, glycerol consumption rate and oxygen uptake rate were constrained to 20 mmol/gDCW/h and 5 mmol/gDCW/h, respectively. In order to simulate the in silico model more accurately, the limits of uptake rates and secretion rates for some metabolites, including amino acids, organic acids (acetic acid, formic acid, lactic acid, pyruvic acid, and succinic acid), and alcohols (ethanol and acetoin), were constrained by experimentally measured flux values. Likewise, the limits associated with secretion for some metabolites, which were not produced during fermentation like amino acids, were constrained to zero. To make a 3D mesh plot graph as a continuous surface for in silico flux solution spaces, the cell growth rate was maximized while gradually increasing the diols production rate and byproducts formation rate, respectively, from their minimal flux values to maximal flux values. The effect of diols production rate in response to varying oxygen uptake rate was examined by flux response analysis [24]. The 1,3-PD and 2,3-BD production rates, as objective function, were maximized and minimized, respectively, according to the changes of oxygen uptake rate from 0 to 20 mmol/gDCW/h with a 20 mmol/gDCW/h glycerol uptake rate. At the same time, the cell growth rate was constrained to 90% of optimal cell growth value for each oxygen condition to release its strict flux solution space. On the other hand, the NADH formation was investigated by in silico flux-sum, which is the cluster of either all ingoing or outgoing fluxes through a metabolite [15].

Bacterial strain and strain development

Klebsiella pneumoniae KCTC12133BP was used as a host for the development of various knockout mutant strains in this study. In-frame deletions were carried out based on homologous recombination using overlap polymerase chain reaction (PCR) products. The overlap product of the two fragments, which consisted of ~500 bp upstream and downstream of the target gene, was amplified and overlapped by PCR. The fragment was cloned in a chloramphenicol-resistant pKGS plasmid (Kim et al. 2013) containing a *sacB* counter-selection marker. The plasmid was transformed into competent cells of the *K. pneumoniae* strain by electroporation. The colonies were then selected in Luria–Bertani (LB) plates at 42 °C with chloramphenicol (25 mg/L), and the integrated cassette was cured by *sacB* expression under sucrose pressure. Integration and excision were confirmed in all mutants by PCR screening using genome-specific primers.

Culture medium and fermentation conditions

Culture medium used in batch and fed-batch fermentations contained (per liter): yeast extract (Becton–Dickinson, Le Pont de Claix, France), 1 g; $MgSO_4 \cdot 7H_2O$, 0.2 g; $(NH_4)_2SO_4$, 2.0 g; K_2HPO_4, 3.4 g; KH_2PO_4, 1.3 g; $CaCl_2 \cdot 2H_2O$, 0.02 g; trace metal solution, 1 mL; Fe solution, 1 mL. The trace metal solution contained (per liter): $ZnCl_2$, 0.07 g; $MnCl_2 \cdot 4H_2O$, 0.1 g; H_3BO_3, 0.06 g; $CoCl_2 \cdot 4H_2O$, 0.2 g; $CuCl_2 \cdot 2H_2O$, 0.02 g; $NiCl_2 \cdot 6H_2O$, 0.025 g; $Na_2MoO_4 \cdot 2H_2O$, 0.035 g; HCl, 4 mL. The Fe solution contained (per liter): $FeSO_4 \cdot 7H_2O$, 5 g; HCl, 4 mL. For inoculum preparation, the suspended cells from single colonies on LB agar (Difco Laboratories, Detroit, MI) plates were precultured in 20-mL test tubes containing 5 mL LB medium at 37 °C for 5 h. One milliliter of the preculture was then transferred to a 500-mL Erlenmeyer flask containing 300 mL LB medium and cultivated to an optical density of 1.5–2.0 at 600 nm (OD_{600}). The tube and flask cultivations

were conducted in a rotary shaker at 150 rpm and 37 °C (JEIO Tech. Co. SI-900R). Three hundred milliliter of the seed culture was then transferred to a 5-L bioreactor.

Lab-scale fed-batch fermentations were performed in a 5-L BIOFLO and CELLIGEN 310 bioreactor (New Brunswick. Scientific Co., Edison, NJ, USA) containing 3 L of culture medium. The bioreactor was continuously aerated through a 0.2-μm membrane filter at a flow rate of 0.5 vvm (air volume/working volume/minute). The temperature was maintained at 37 °C. The pH was controlled at 6.0 ± 0.1 by the automatic feeding of NH_4OH. Foaming was controlled by the addition of Antifoam 289 (Sigma, St. Louis, MO, USA). All bioreactor experiments were performed at least three times independently, and the representative results are shown in figures. Pilot-scale fed-batch fermentations were performed in a 5000-L bioreactor containing 3000 L of culture medium under the same conditions as lab-scale fermentations except for the agitation speed. Samples were periodically taken for the measurement of OD_{600} as well as for the determination of metabolites. After centrifugation at 13,200×*g* for 5 min, the resulting supernatant was used to determine the concentrations of glycerol, 1,3-PD, 2,3-BD, and byproducts.

Analytical methods

Cell growth was monitored by measuring the OD of the culture broth at 600 nm (UV–Vis spectrophotometer; DR5000, HACH Company, CO, USA). Cell concentration, defined as dry cell weight (DCW) per liter of culture broth, was then calculated by using a predetermined calibration curve (1 OD_{600} = 0.5425 gDCW/L). The concentration of glycerol, 1,3-PD, 2,3-BD, lactic acid, ethanol, acetic acid, formic acid, acetoin, and succinic acid was determined with high-performance liquid chromatography (HPLC, Agilent 1260 series, Agilent Technologies, Waldbronn, Germany) equipped with UV/VIS and RI detectors and Aminex HPX-87H column (300 mm × 7.8 mm, Bio-Rad, Hercules, CA, USA). The column was isocratically eluted with 0.01 N H_2SO_4 at 80 °C and a flow rate of 0.6 mL/min.

Results and discussion

In silico single gene knockout simulation and investigation of *K. pneumoniae* wild-type and *ΔldhA* strains based on in silico analysis

Klebsiella pneumoniae wild-type strain produced 1,3-PD and 2,3-BD along with several byproducts, including lactic acid, succinic acid, ethanol, formic acid, acetic acid, and acetoin, under microaerobic conditions [12, 17] (Figs. 1, 2). For enhanced 1,3-PD and 2,3-BD co-production, the formation of byproducts should be reduced, after which the remaining metabolic fluxes from carbon sources should be redirected toward the synthesis of 1,3-PD and 2,3-BD. The best candidate for gene knockout was based on the criteria of maximizing 1,3-PD and 2,3-BD production rates, minimizing byproducts formation rates, and minimizing cell growth retardation. The knockout of the *ldhA* gene encoding lactate dehydrogenase, which converts pyruvic acid into lactic acid with NADH oxidation, was targeted by in silico simulation with top priority to eliminate the formation of lactic acid. Then, the iYL1228 model investigated the metabolic characteristics of the *ldhA* gene knockout mutant by examining the changes of flux solution space compared with those of the wild-type strain. In the *ldhA* gene knockout mutant, the optimal point shifted to an increased production of 1,3-PD and 2,3-BD but to a decreased formation of byproducts, especially lactic acid.

The predictions were validated by fed-batch fermentations of *K. pneumoniae* wild-type and *ldhA* gene knockout strains (Fig. 2). *K. pneumoniae* wild-type strain formed 42.1 g/L of lactic acid and produced 42.7 g/L of 1,3-PD and 1.8 g/L of 2,3-BD (44.5 g diols/L, 0.92 g diols/L/h). In contrast, the *ldhA* gene knockout mutant dramatically decreased the lactic acid formation to about 0 g/L and increased 1,3-PD and 2,3-BD production to 71.8 and 30.1 g/L (101.9 g diols/L, 1.8 g diols/L/h), respectively (Fig. 2c, d; Table 1). On the other hand, cell growth and glycerol uptake rates of the *ldhA* gene knockout mutant were maintained in comparison with those of the wild-type strain. This is mainly because the redox balance of NAD^+/NADH was not disrupted by the knockout of the *ldhA* gene. The inactivation of lactate dehydrogenase forming lactic acid with the oxidation of NADH seemed to be compensated with 1,3-PD dehydrogenase and 2,3-BD dehydrogenase producing 1,3-PD and 2,3-BD, respectively, with the oxidation of NADH. Moreover, *ldhA* gene knockout regulated the metabolic flux toward the oxidative pathway of glycerol metabolism, and therefore, the significantly increased pyruvic acid pool seemed to redirect the metabolic flux to 2,3-BD synthesis. When we investigated the in silico flux solution space of the *ldhA* gene knockout mutant in Fig. 2, it appeared that more improvements for 1,3-PD and 2,3-BD co-production could be made by further genetic manipulation. In particular, the fermentation results of the *ldhA* gene knockout mutant in Fig. 2 suggested the construction of a mutant, which would prevent the formation of succinic acid (7.1 g/L) and ethanol (2.9 g/L).

In silico single gene knockout simulation and investigation of *K. pneumoniae ΔldhA Δmdh* strains based on in silico analysis

The *K. pneumoniae ΔldhA* strain still produced somewhat high amounts of byproducts, especially succinic acid

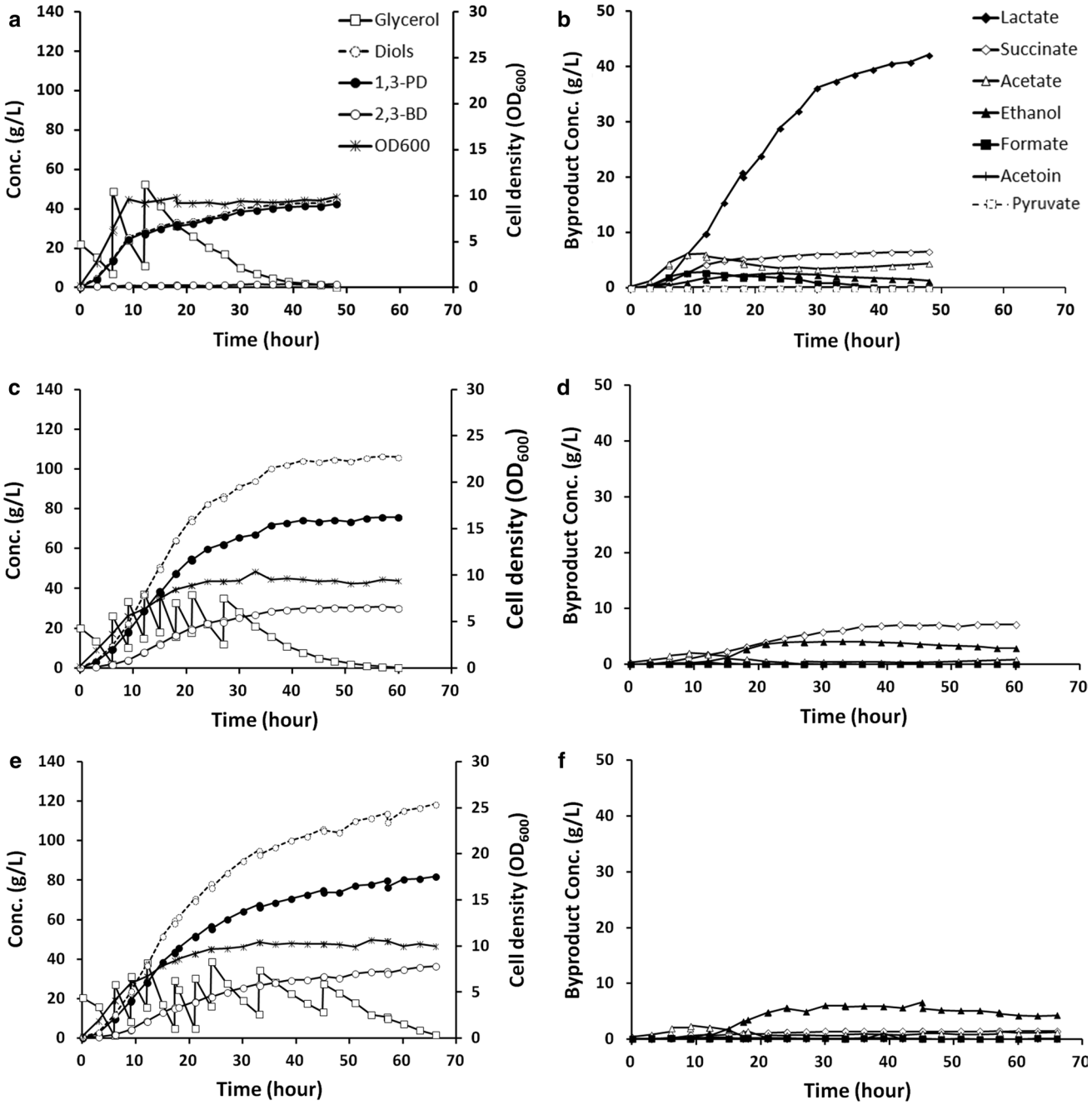

Fig. 2 Fed-batch fermentation results for **a** and **b** *K. pneumoniae* wild-type, **c** and **d** *K. pneumoniae ΔldhA* and **e** and **f** *K. pneumoniae ΔldhA Δmdh* strains. Fermentations were performed with a working volume of 3 L at 37 °C and 200 rpm. The aeration rate was maintained at 0.5 vvm, and pH was controlled at 6.0 by the automatic feeding of NH_4OH. *Symbols* in fermentation profiles denote the concentration of glycerol (*open squares*), diols (*dotted open circles*), 1,3-PD (*filled circles*), 2,3-BD (*open circles*), cell mass (*asterisks*), lactic acid (*filled diamonds*), succinic acid (*open diamonds*), acetic acid (*open triangles*), ethanol (*filled triangles*), formic acid (*filled squares*), acetoin (*crosses*), and pyruvate (*dotted open squares*)

(7.1 g/L) and ethanol (2.9 g/L). Although the optimal status of in silico flux solution space of the *ldhA* knockout strain was shifted to increasing 1,3-PD and 2,3-BD co-production compared with that of the wild-type strain, the formation rates of the byproducts in the *ldhA* knockout strain were still higher than 3 mmol/gDCW/h (Fig. 1c). This in silico analysis implies that further strain improvement is possible (Fig. 1). Since ethanol can be separated in a downstream process much easier than succinic acid due to its low boiling point (78.4 °C), we focused on decreasing the succinic

Table 1 Fed-batch fermentation results of *K. pneumoniae* wild-type and its knockout mutants

Strain	Bioreactor (L)	Agitation (rpm)	Carbon source	Diols titer (g/L)	Diols yield (g/g glycerol)	Diols productivity (g/L/h)	Byproducts (g/L)			
							Lactate	Succinate	Ethanol	Acetate
Wild-type	5	200	Glycerol	44.5 ± 2.2	0.42 ± 0.033	0.92 ± 0.033	42.1 ± 0.30	6.5 ± 0.31	1.3 ± 0.26	4.4 ± 0.40
ΔldhA	5	200	Glycerol	101.9 ± 2.1	0.58 ± 0.025	1.8 ± 0.025	0	7.1 ± 0.50	2.9 ± 0.31	0.9 ± 0.51
ΔldhA Δmdh	5	200	Glycerol	118.5 ± 1.9	0.63 ± 0.019	1.8 ± 0.019	0	1.4 ± 0.25	4.2 ± 0.55	1.2 ± 0.29
ΔldhA ΔbudABC	5	200	Glycerol	31.5 ± 2.5	0.33 ± 0.034	0.46 ± 0.041	2.5 ± 1.38	9.2 ± 2.45	1.7 ± 1.21	5.4 ± 1.23
ΔldhA Δmdh	5	300	Glycerol	125.0 ± 3.6	0.65 ± 0.028	2.0 ± 0.027	0	1.1 ± 0.12	4.7 ± 0.21	1.7 ± 0.17
ΔldhA Δmdh	5	400	Glycerol	114.5 ± 2.8	0.60 ± 0.021	1.8 ± 0.022	0	1.5 ± 0.21	9.3 ± 0.86	2.4 ± 0.69
ΔldhA Δmdh	5	300	Crude Glycerol	130.7 ± 4.5	0.65 ± 0.027	2.1 ± 0.036	0	1.7 ± 0.52	3.9 ± 1.87	2.1 ± 0.83
ΔldhA Δmdh	5000	70	Crude Glycerol	114.2	0.60	2.2	0	1.5	6.8	1.7

All bioreactor experiments except for pilot-scale fermentation were performed at least three times independently

acid formation. Moreover, in silico knockout simulation indicated that the growth can be retarded extremely by blocking the pathway of ethanol formation. The inactivation of alcohol dehydrogenase oxidizing NADH seemed to increase the accumulation of pyruvic acid too much, which can inhibit the glycolytic pathway and glycerol uptake [10, 34]. As a result of simulation, the *mdh* gene encoding malate dehydrogenase was selected as a top priority knockout candidate for 1,3-PD and 2,3-BD co-production. The metabolic characteristics of *K. pneumoniae ΔldhA Δmdh* strain were investigated by in silico flux solution space (Fig. 1d). The additional knockout of *mdh* gene dramatically decreased the formation rate of succinic acid to less than 0.5 mmol/gDCW/h and redirected the remaining metabolic fluxes into 1,3-PD and 2,3-BD synthesis. In addition, no apparent cell growth retardation occurred by deleting the *mdh* gene. Malate dehydrogenase is known to be involved in the reduction of oxaloacetic acid to malic acid, which is further converted to fumaric acid which forms succinic acid with the oxidation of NADH to NAD^+. The knockout of the *mdh* gene seemed to effectively increase the pool of NADH (important cofactor and precursor for 1,3-PD and 2,3-BD synthesis) redirected into 1,3-PD and 2,3-BD co-production, without the disruption of redox balance and reduction of growth rate.

Based on the in silico predictions and observations, *K. pneumoniae ΔldhA Δmdh* strain was constructed. Fed-batch fermentations of *K. pneumoniae ΔldhA Δmdh* strain were performed at 200 rpm and 37 °C (Fig. 2). As the in silico predictions, succinic acid formation was decreased to less than 1 g/L with the *K. pneumoniae ΔldhA Δmdh* strain, while the *ldhA* knockout strain formed more than 7 g/L of succinic acid (Fig. 2e, f). The *K. pneumoniae ΔldhA Δmdh* strain produces about 82.0 g/L of 1,3-PD and 36.6 g/L of 2,3-BD (118.5 g diols/L, 1.8 g diols/L/h). This is more than 2.7 times and 1.2 times higher than diols produced by the wild-type (44.5 g/L of diols) and the *ldhA* knockout (101.9 g/L of diols) strains, respectively (Fig. 2; Table 1). In particular, the production yield of diols by the *K. pneumoniae ΔldhA Δmdh* strain on glycerol was much higher (0.63 g diols/g glycerol) than those of the wild-type (0.42 g diols/g glycerol) and *ldhA* knockout (0.58 g diols/g glycerol) strains.

In order to explain the advantage of co-production of 1,3-PD and 2,3-BD clearly, we developed a mutant with the genes *ldhA*, *budA* (acetolactate decarboxylase), *budB* (acetolactate synthase), and *budC* (2,3-BD dehydrogenase) deleted. Fed-batch fermentations of *K. pneumoniae ΔldhA ΔbudABC* strain were performed at 200 rpm and 37 °C (Fig. 3). Due to the elimination of the pathway for 2,3-BD synthesis, no 2,3-BD was produced, while pyruvic acid was formed more than 15 g/L with the *K. pneumoniae ΔldhA ΔbudABC* strain. By deleting the *budABC* genes,

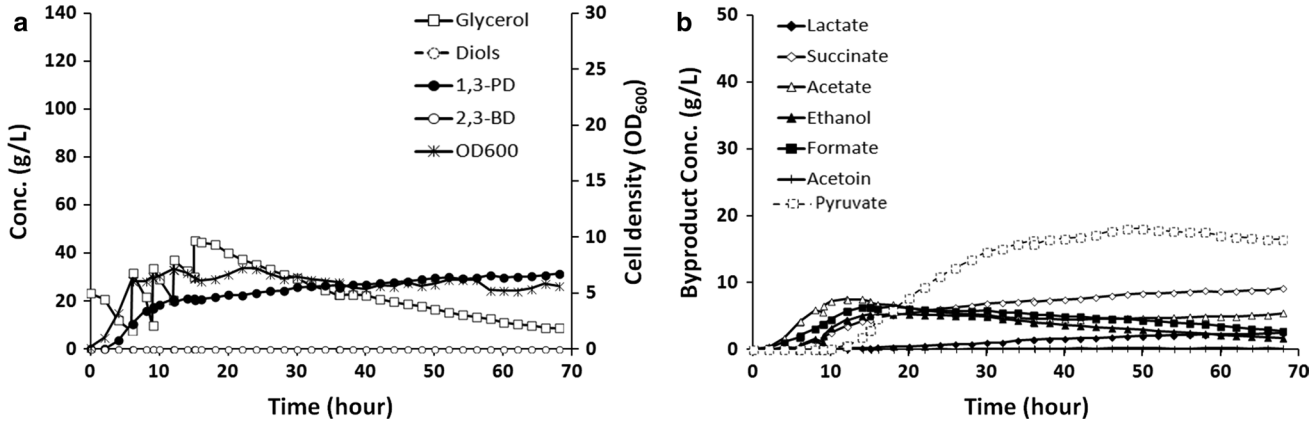

Fig. 3 Fed-batch fermentation results for **a** and **b** *K. pneumoniae ΔldhA ΔbudABC* strain. Fermentations were performed with a working volume of 3 L at 37 °C and 200 rpm. The aeration rate was maintained at 0.5 vvm, and pH was controlled at 6.0 by the automatic feeding of NH_4OH. *Symbols* in fermentation profiles denote the concentration of glycerol (*open squares*), diols (*dotted open circles*), 1,3-PD (*filled circles*), 2,3-BD (*open circles*), cell mass (*asterisks*), lactic acid (*filled diamonds*), succinic acid (*open diamonds*), acetic acid (*open triangles*), ethanol (*filled triangles*), formic acid (*filled squares*), acetoin (*crosses*), and pyruvate (*dotted open squares*)

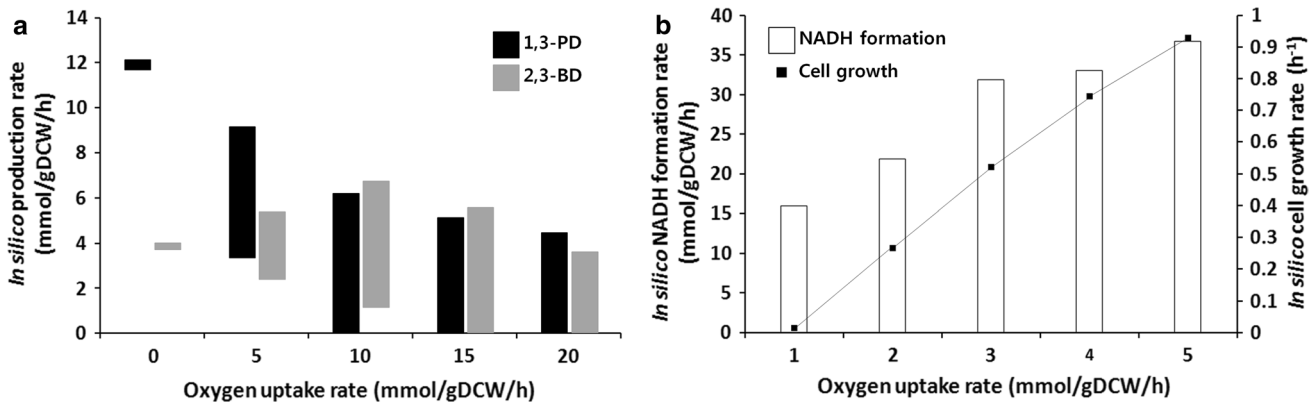

Fig. 4 In silico predictions to examine the response of carbon flux distributions varying oxygen uptake rate from 0 to 20 mmol/gDCW/h in *K. pneumoniae ΔldhA Δmdh* strain. **a** Changes of flux solution spaces for 1,3-PD and 2,3-BD production. **b** Changes of optimal cell growth rate and the flux-sum of NADH formation. The *bars* indicate the ranges of in silico metabolic fluxes computed by flux response analysis. *Symbols* denote the in silico metabolic flux of 1,3-PD (*filled black squares*), 2,3-BD (*filled gray squares*), NADH (*open squares*), and cell growth (*black dots*)

cell growth and glycerol uptake rates were retarded apparently. Consequently, 1,3-PD production was decreased to 31.5 g/L, which is about half of 1,3-PD produced by the *ldhA* knockout strain. The accumulation of pyruvic acid seems to inhibit glycolytic pathway and glycerol uptake [10, 34].

Improvement of diols productivity by changing agitation speeds

Previous studies showed that the production of 1,3-PD and 2,3-BD by *Klebsiella* strains was strongly affected with the variations in agitation speed and aeration rate during fermentation [11, 18, 24, 25, 33]. In order to gain an insight into the effect of oxygen uptake rate on 1,3-PD and 2,3-BD production in *K. pneumoniae*, the oxygen uptake rate was perturbed by constraints-based flux analysis between 0 and 20 mmol/gDCW/h and glycerol uptake rate was fixed to 20 mmol/gDCW/h. Given the fact that multiple equivalent solutions of intracellular metabolic fluxes can be computed for the same state [19, 23], we should investigate the changes of in silico flux solution spaces for 1,3-PD and 2,3-BD production by flux response analysis (Fig. 4). Likewise, the NADH formation calculated by flux sum, which is defined as the half of the summation of all consumption and generation rate around a particular metabolite under pseudo-steady states [15], supported the changes of carbon flux distribution. As shown in Fig. 4, the calculated cell

growth rate increased as the oxygen uptake rate was raised to 0 and 20 mmol/gDCW/h. Consequently, the total diols production flux decreased, but 2,3-BD production ratio of total diols and NADH formation rate increased with increasing oxygen uptake rate (Fig. 4). In the higher oxygen level, the glycerol taken up was redirected to the oxidative pathway which favored the glycolysis and TCA cycle pathway related to biomass synthesis, energy generation, and pyruvate synthesis (a most important precursor for 2,3-BD synthesis). Additionally, the in silico prediction showed that the optimal oxygen level existed on 1,3-PD and 2,3-BD production. In the consideration of their productivity and yield resulted from the in silico simulation, the optimal oxygen level is nearly 5 mmol/gDCW/h of oxygen uptake rate. These results indicated that deficient or excessive oxygen exposure could impair the enhanced production of 1,3-PD and 2,3-BD.

In order to improve the overall diols productivity of *K. pneumoniae ΔldhA Δmdh* strain, agitation speeds were varied from 200 to 400 rpm to determine its effect on 1,3-PD and 2,3-BD co-production and cell growth (Fig. 5). The aeration rate was fixed at 0.5 vvm in this study because there are technical and economic limitations to increasing the aeration rate in large-scale fermentations. As shown in Fig. 5, the final diols concentration and productivity increased from 118.5 to 125 g/L and 1.8 to 2.0 g/L/h by raising the agitation speed from 200 to 300 rpm. No further increase in diols production was observed at 400 rpm (Table 1). The highest diols yield of 0.65 g diols/g glycerol was also achieved at the agitation speed of 300 rpm.

On the other hand, the highest glycerol consumption was observed at 400 rpm with more glycerol being used to synthesize biomass, not 1,3-PD and 2,3-BD. The specific cell growth rate (μ) and final cell density (OD_{600}) at 400 rpm were increased by more than 1.5- and twofold, respectively, compared with those at 200 rpm. The total diols concentration was lower at 400 rpm (113.9 g/L) than at 300 rpm (125 g/L) and 200 rpm (118.5 g/L). However, the concentration of 2,3-BD (50.1 g/L, 44% of total diols) at 400 rpm was much higher than the 2,3-BD concentrations at 300 rpm (43.6 g/L, 35% of total diols) and 200 rpm (36.6 g/L, 31% of total diols) (Table 1; Fig. 5). These results are a strong indication that the glycerol taken up at the higher agitation speed was redirected to the oxidative pathway of glycerol metabolism. Many researchers have reported that there are optimal aeration and agitation conditions for 1,3-PD and 2,3-BD production [11, 18, 24, 25, 33], and Kosaric et al. [13] demonstrated the rapid

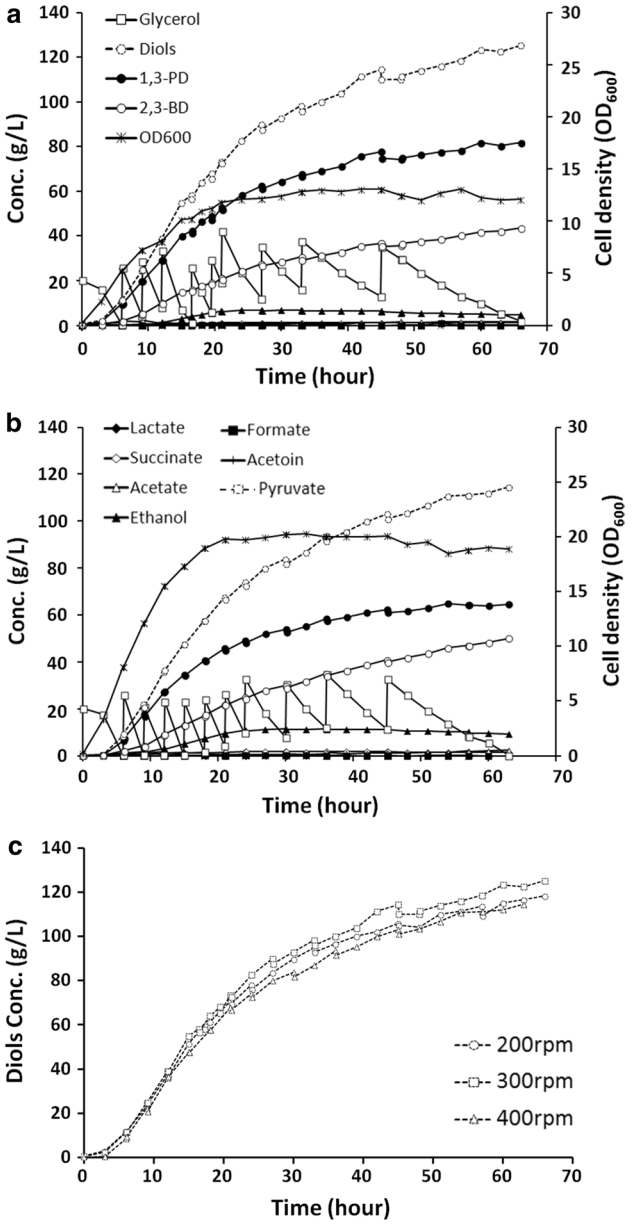

Fig. 5 Fed-batch fermentations of *K. pneumoniae ΔldhA Δmdh* strain at different agitation speeds. Fermentation results of **a** 300 rpm, and **b** 400 rpm. **c** Comparison of 2,3-BD production profile for different agitation speeds. Fermentations were performed with a working volume of 3 L at 37 °C. The aeration rate was maintained at 0.5 vvm, and pH was controlled at 6.0 by the automatic feeding of NH_4OH. *Symbols* in fermentation profiles denote the concentration of glycerol (*open squares*), diols (*dotted open circles*), 1,3-PD (*filled circles*), 2,3-BD (*open circles*), cell mass (*asterisks*), lactic acid (*filled diamonds*), succinic acid (*open diamonds*), acetic acid (*open triangles*), ethanol (*filled triangles*), formic acid (*filled squares*), acetoin (*crosses*), and pyruvate (*dotted open squares*)

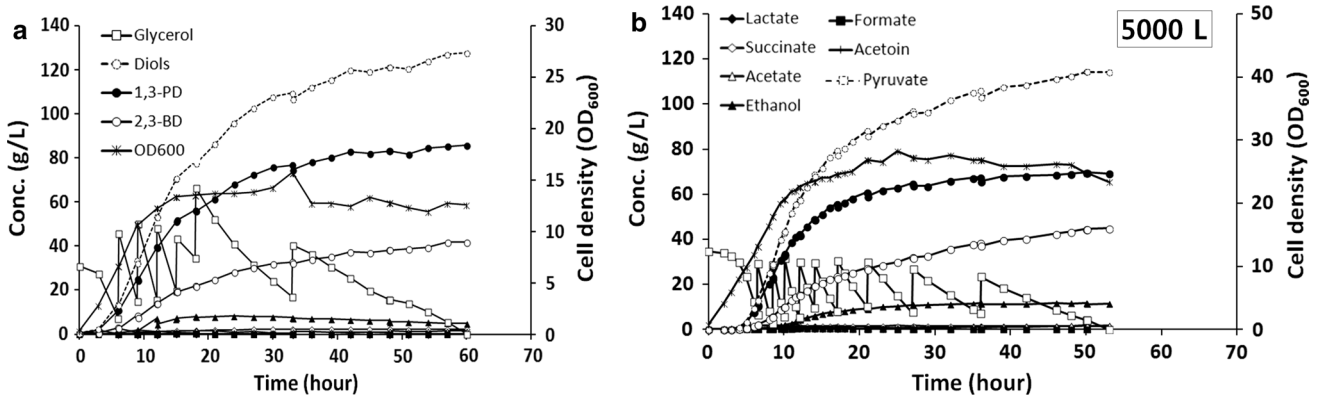

Fig. 6 **a** Fed-batch fermentations of *K. pneumoniae ΔldhA Δmdh* strain by using crude glycerol and **b** pilot-scale fed-batch fermentation of *K. pneumoniae ΔldhA Δmdh* strain (5000 L). Laboratory-scale fermentation was performed with a working volume of 3 L at 37 °C and 200 rpm. Pilot-scale fermentation was performed with a working volume of 3000 L at 37 °C and 100 rpm. The aeration rate was maintained at 0.5 vvm, and pH was controlled at 6.0 by the automatic feeding of NH_4OH. *Symbols* in fermentation profiles denote the concentration of glycerol (*open squares*), diols (*dotted open circles*), 1,3-PD (*filled circles*), 2,3-BD (*open circles*), cell mass (*asterisks*), lactic acid (*filled diamonds*), succinic acid (*open diamonds*), acetic acid (*open triangles*), ethanol (*filled triangles*), formic acid (*filled squares*), acetoin (*crosses*), and pyruvate (*dotted open squares*)

inactivation of alpha-acetolactate synthase in 2,3-BD synthesis pathway under a high oxygen supply [13].

Pilot-scale fermentation by using crude glycerol

To evaluate the industrial fermentative co-production of 1,3-PD and 2,3-BD, pilot-scale fermentation was carried out using crude glycerol in a 5000-L bioreactor (Fig. 6). First, the feasibility of using crude glycerol obtained from the industrial biodiesel plant (GSBio, Korea, Yeosu-city, Jeollanam-do, Korea) was tested in a 5-L bioreactor. Crude glycerol contained (per 100 g): glycerol, 83.1 g; water, 8.6 g; Na^{2+}, 2.4 g; Cl^{-}, 2.3 g; matter organic non-glycerol, 1.1 g; and ash, 2.5 g. *K. pneumoniae ΔldhA Δmdh* strain produced 86.1 g/L of 1,3-PD and 44.6 g/L of 2,3-BD (130.7 g diols/L, 0.65 g diols/g glycerol, 2.1 g diols/L/h) from crude glycerol. These results are quite similar to the results obtained using high-quality guaranteed reagent grade glycerol (99%, Junsei Chemical, Chuo-ku, Tokyo, Japan), 125 g diols/L, 0.65 g/g glycerol, 2.0 g diols/L/h (Table 1). Therefore, it might be concluded that crude glycerol can be used for the fermentative co-production of 1,3-PD and 2,3-BD without prior purification.

The pH (6.0), temperature (37 °C), and aeration rate (0.5 vvm) used in the 5-L bioreactor were easily set up in the 5000-L bioreactor. In general, the concentration of dissolved oxygen (DO) is dependent on the mechanical parts related to the agitation system such as reactor shape, baffle type, and motor type. Thus, the optimal agitation speed in the 5000-L bioreactor was determined at 70 rpm by comparing the DO concentration with that measured at 300 rpm in the 5-L bioreactor (data not shown). In the 5000-L bioreactor, *K. pneumoniae ΔldhA Δmdh* strain produced about 70.1 g/L of 1,3-PD and 44.1 g/L of 2,3-BD (114.2 g diols/L, 0.60 g/g glycerol, 2.2 g diols/L/h) using crude glycerol (Table 1; Fig. 6). Although the final concentration of diols and its yield on glycerol were slightly lower than those obtained in the 5-L bioreactor, these results seem to support that the fed-batch fermentation of crude glycerol would be suitable for the industrial co-production of 1,3-PD and 2,3-BD.

Conclusions

To improve the potential of *K. pneumoniae* for industrial applications, a *K. pneumoniae ΔldhA Δmdh* strain was developed for 1,3-PD and 2,3-BD production based on in silico aided metabolic engineering. In silico analyses based on genome-scale metabolic model predicted that the inactivation of *ldhA* and *mdh* genes reduced effectively the formation of byproducts and enhanced the production of 1,3-PD and 2,3-BD production without cell growth retardation. The mutant was successfully evaluated by batch fermentations with a high yield of diols compared with the wild-type and *ldhA* knockout strains. In order to improve the productivity of diols, the effect of oxygen level on 1,3-PD and 2,3-BD production was investigated by in silico metabolic flux analysis. Then, the agitation speeds in batch fermentations were varied from 200 to 400 rpm. Subsequently, the fed-batch fermentation with the agitation speed of 300 rpm was performed by using high-quality guaranteed reagent grade glycerol and crude glycerol. The high concentration, yield, and productivity of diols were achieved by the

lab-scale fed-batch fermentation up to 130 g/L, 0.65 g/g, and 2.1 g/L/h, respectively. In order to evaluate the industrial fermentation of *K. pneumoniae ΔldhA Δmdh* strain for 1,3-PD and 2,3-BD production, pilot-scale fermentation (5000-L bioreactor) was carried out using crude glycerol. The pilot-scale fed-batch fermentation of the *K. pneumoniae ΔldhA Δmdh* strain could achieve up to 114 g/L, 0.60 g/g, and 2.2 g/L/h of diols. This is an example showing the effectiveness of systems metabolic engineering for development of industrial microorganism and the importance of agitation speed during fermentation for 1,3-PD and 2,3-BD production in *K. pneumoniae* strain. Likewise, it is expected that the strategies used in this study are applicable to develop industrial processes of the other products.

Acknowledgements This work was supported by the Industrial Strategic Technology Development Program (No. 10050407) funded by the Ministry of Trade, Industry and Energy (MOTIE, Korea).

References

1. Arasu MV, Kumar V, Ashok S, Hyohak S, Rathnasingh C, Lee HJ, Seung D, Park S (2011) Isolation and characterization of the new *Klebsiella pneumoniae* J2B strain showing improved growth characteristics with reduced lipopolysaccharide formation. Biotech Bioproc Eng 16:1134–1143
2. Biebl H, Zeng AP, Menzel K, Deckwer WD (1998) Fermentation of glycerol to 1,3-propanediol and 2,3-butanediol by *Klebsiella pneumoniae*. Appl Microbiol Biotechnol 50:24–29
3. Celińska E, Grajek W (2009) Biotechnological production of 2,3-butanediol—current state and prospects. Biotechnol Adv 27:715–725
4. Cui YL, Zhou JJ, Gao LR, Zhu CQ, Jiang X, Fu SL, Gong H (2014) Utilization of excess NADH in 2,3-butanediol-deficient *Klebsiella pneumoniae* for 1,3-propanediol production. J Appl Microbiol 117:690–698
5. da Silva GP, Mack M, Contiero J (2009) Glycerol: a promising and abundant carbon source for industrial microbiology. Biotechnol Adv 27:30–39
6. Durgapal M, Kumar V, Yang TH, Lee HJ, Seung D, Park S (2014) Production of 1,3-propanediol from glycerol using the newly isolated *Klebsiella pneumoniae* J2B. Bioresour Technol 159:223–231
7. Edwards JS, Ramakrishna R, Schilling CH, Palsson BO (1999) Metabolic flux balance analysis. In: Lee SY, Papoutsakis ET (eds) Metabolic engineering. Marcel Dekker, New York
8. Garg SK, Jain A (1995) Fermentative production of 2,3-butanediol: a review. Bioresour Technol 51:103–109
9. Gombert AK, Nielsen J (2000) Mathematical modelling of metabolism. Curr Opin Biotechnol 11:180–186
10. Guo X, Cao C, Wang Y, Li C, Wu M, Chen Y, Zhang C, Pei H, Xiao D (2014) Effect of the inactivation of lactate dehydrogenase, ethanol dehydrogenase, and phosphotransacetylase on 2,3-butanediol production in *Klebsiella pneumoniae* strain. Biotechnol Biofuels 7:44
11. Ji XJ, Huang H, Du J, Zhu JG, Ren LJ, Hu N, Li S (2009) Enhanced 2,3-butanediol production by *Klebsiella oxytoca* using a two-stage agitation speed control strategy. Bioresour Technol 100:3410–3414
12. Jung MY, Mazumdar S, Shin SH, Yang KS, Lee J, Oh MK (2014) Improvement of 2,3-butanediol yield in *Klebsiella pneumoniae* by deletion of the pyruvate formate-lyase gene. Appl Environ Microbiol 80:6195–6203
13. Kosaric N, Magee RJ, Blaszczyk R (1992) Redox potential measurement for monitoring glucose and xylose conversion by *K. pneumoniae*. Chem Biochem Eng Q 6:145–152
14. Kumar V, Durgapal M, Sankaranarayanan M, Somasundar A, Rathnasingh C, Song H, Seung D, Park S (2016) Effects of mutation of 2,3-butanediol formation pathway on glycerol metabolism and 1,3-propanediol production by *Klebsiella pneumoniae* J2B. Bioresour Technol 214:432–440
15. Lakshmanan M, Kim TY, Chung BK, Lee SY, Lee DY (2015) Flux-sum analysis identifies metabolite targets for strain improvement. BMC Syst Biol 9:73
16. Liao YC, Huang TW, Chen FC, Charusanti P, Hong JS, Chang HY, Tsai SF, Palsson BO, Hsiung CA (2011) An experimentally validated genome-scale metabolic reconstruction of *Klebsiella pneumoniae* MGH 78578, iYL1228. J Bacteriol 193:1710–1717
17. Lin J, Zhang Y, Xu D, Xiang G, Jia Z, Fu S, Gong H (2016) Deletion of *poxB*, *pta*, and *ackA* improves 1,3-propanediol production by *Klebsiella pneumoniae*. Appl Microbiol Biotechnol 100:2775–2784
18. Ma BB, Xu XL, Zhang GL, Wang LW, Wu M, Li C (2009) Microbial production of 1,3-propanediol by *Klebsiella pneumoniae* XJPD-Li under different aeration strategies. Appl Biochem Biotechnol 152:127–134
19. Mahadevan R, Schilling CH (2003) The effects of alternate optimal solutions in constraint-based genome-scale metabolic models. Metab Eng 5:264–276
20. Oh BR, Seo JW, Heo SY, Hong WK, Luo LH, Kim S, Park DH, Kim CH (2012) Optimization of culture conditions for 1,3-propanediol production from glycerol using a mutant strain of *Klebsiella pneumoniae*. Appl Biochem Biotechnol 166:127–137
21. Orth JD, Conrad TM, Na J, Lerman JA, Nam H, Feist AM, Palsson BO (2011) A comprehensive genome-scale reconstruction of *Escherichia coli* metabolism—2011. Mol Syst Biol 7:535
22. Park JM, Kim TY, Lee SY (2009) Constraints-based genome-scale metabolic simulation for systems metabolic engineering. Biotechnol Adv 27:979–988
23. Park JM, Kim TY, Lee SY (2010) Prediction of metabolic fluxes by incorporating genomic context and flux-converging pattern analyses. Proc Natl Acad Sci USA 107:14931–14936
24. Park JM, Song H, Lee HJ, Seung D (2013) Genome-scale reconstruction and in silico analysis of *Klebsiella oxytoca* for 2,3-butanediol production. Microb Cell Fact 12:20
25. Park JM, Song H, Lee HJ, Seung D (2013) In silico aided metabolic engineering of *Klebsiella oxytoca* and fermentation optimization for enhanced 2,3-butanediol production. J Ind Microbiol Biotechnol 40:1057–1066
26. Rathnasingh C, Kim DK, Song H, Lee HJ, Seung D, Park S (2012) Isolation and characterization of a new mucoid-free *Klebsiella pneumoniae* strain for 2,3-butanediol production. Afr J Biotechnol 11:11252–11261
27. Rathnasingh C, Park JM, Kim DK, Song H, Chang YK (2016) Metabolic engineering of *Klebsiella pneumoniae* and in silico investigation for enhanced 2,3-butanediol production. Biotechnol Lett 38:975–982
28. Ryu CM, Farag MA, Hu CH, Reddy MS, Kloepper JW, Paré PW (2004) Bacterial volatiles induce systemic resistance in *Arabidopsis*. Plant Physiol 134:1017–1026
29. Ryu CM, Farag MA, Hu CH, Reddy MS, Wei HX, Paré PW, Kloepper JW (2003) Bacterial volatiles promote growth in *Arabidopsis*. Proc Natl Acad Sci USA 100:4927–4932

30. Saxena RK, Anand P, Saran S, Isar J (2009) Microbial production of 1,3-propanediol: recent developments and emerging opportunities. Biotechnol Adv 27:895–913
31. Schuetz R, Kuepfer L, Sauer U (2007) Systematic evaluation of objective functions for predicting intracellular fluxes in *Escherichia coli*. Mol Syst Biol 3:119
32. Varma A, Palsson BO (1994) Metabolic flux balancing: basic concepts, scientific and practical use. Biotechnology 12:994–998
33. Wang Y, Teng H, Xiu Z (2011) Effect of aeration strategy on the metabolic flux of *Klebsiella pneumoniae* producing 1,3-propanediol in continuous cultures at different glycerol concentrations. J Ind Microbiol Biotechnol 38:705–715
34. Williamson JR, Jones EA (1964) Inhibition of glycolysis by pyruvate in relation to the accumulation of citric acid cycle intermediates in the perfused rat heart. Nature 203:1171–1173
35. Xu YZ, Guo NN, Zheng ZM, Ou XJ, Liu HJ, Liu DH (2009) Metabolism in 1,3-propanediol fed-batch fermentation by a D-lactate deficient mutant of *Klebsiella pneumoniae*. Biotechnol Bioeng 104:965–972
36. Yen HW, Li FT, Chang JS (2014) The effects of dissolved oxygen level on the distribution of 1,3-propanediol and 2,3-butanediol produced from glycerol by an isolated indigenous *Klebsiella* sp. Ana-WS5. Bioresour Technol 153:374–378
37. Zeng AP, Sabra W (2011) Microbial production of diols as platform chemicals: recent progresses. Curr Opin Biotechnol 22:749–757
38. Zhu C, Jiang X, Zhang Y, Lin J, Fu S, Gong H (2015) Improvement of 1,3-propanediol production in *Klebsiella pneumoniae* by moderate expression of *puuC* (encoding an aldehyde dehydrogenase). Biotechnol Lett 37:1783–1790